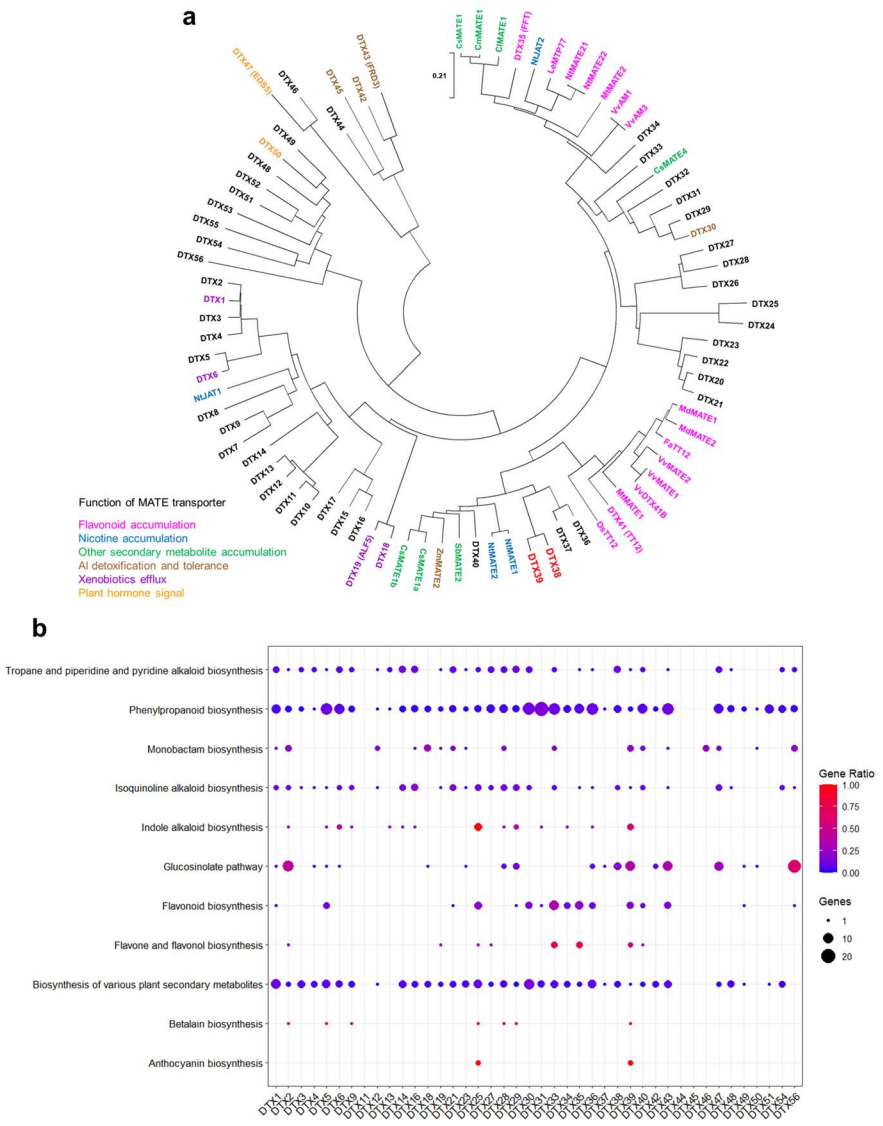

Extended Data Fig. 1. Phylogenetic and co-expression analyses of MATE transporters.
a, Phylogenetic tree of selected plant MATE transporters. Amino acid sequences were aligned using the MUSCLE program with default settings in MEGA-X software. The phylogenetic tree was constructed using the neighbor-joining method. The abbreviations of the proteins are listed in Supplementary Table 3. The scale bar represents evolutionary distance, expressed as the number of substitutions per amino acid. DTX38 and DTX39 are highlighted in red. The other colors are based on the functions of MATE transporters: flavonoid accumulation (magenta), nicotine accumulation (blue), other secondary metabolite accumulation (green), Al detoxification and tolerance (brown), xenobiotics efflux (purple), and plant hormone signaling (orange).
b, Functional enrichment analysis of Arabidopsis MATE transporters. The top 500 co-expressed genes of each MATE transporter were collected using the ATTED-II database, and mapped to the secondary pathways using the KEGG database. The width of the circles represents the number of mapped genes. Colors show the proportion of mapped genes against the total genes associated with the pathway.

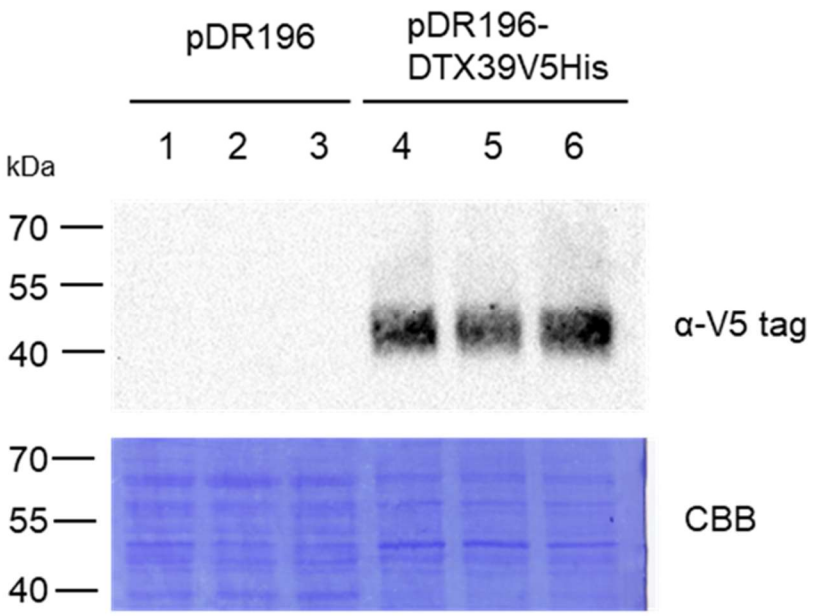

Extended Data Fig. 2. DTX39 protein accumulation in yeast microsomes.
Immunoblot of microsomes (8 μg protein per lane) from transgenic yeast containing empty vector (pDR196) and DTX39 construct (pDR196-DTX39-V5-6×His). The DTX39-V5-6×His protein was detected with the V5 epitope tag antibody. The image shows three independent samples of control (lanes 1 to 3) and DTX39-expressing (lanes 4 to 6) cells. Coomassie blue staining served as a loading control.

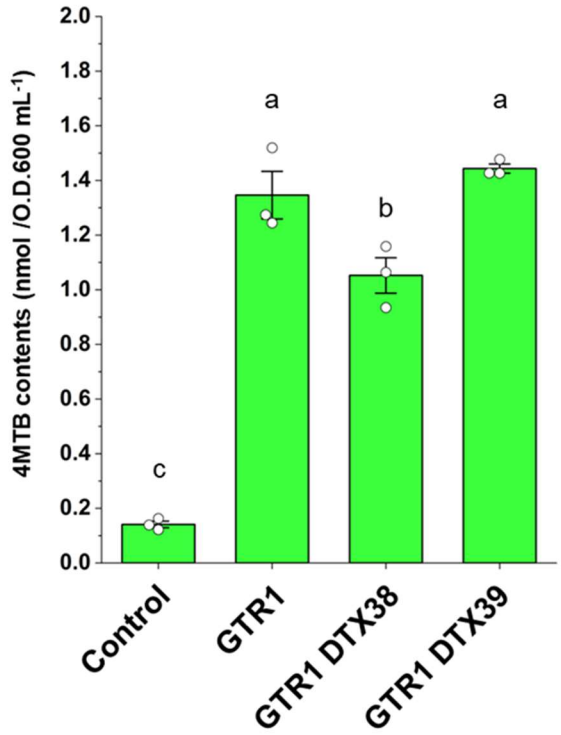

Extended Data Fig. 3. DTX38 and DTX39 expression do not enhance accumulation of exogenously added aliphatic glucosinolate in yeast cells.
Accumulation of exogenously added 4MTB in yeast cells transformed with the empty vector (Control), in cells expressing GTR1, or in cells co-expressing GTR1 and DTX38, or GTR1 and DTX39. We used GTR1 because it exhibits high transport activity toward aliphatic glucosinolates. The chart shows accumulation levels after 2 days of culturing in the presence of 100 µM 4MTB. Error bars represent the standard error (SE) of three independent experiments (n = 3). Different lowercase letters indicate significant differences using one-way ANOVA with a Tukey's HSD test ($p < 0.05$).

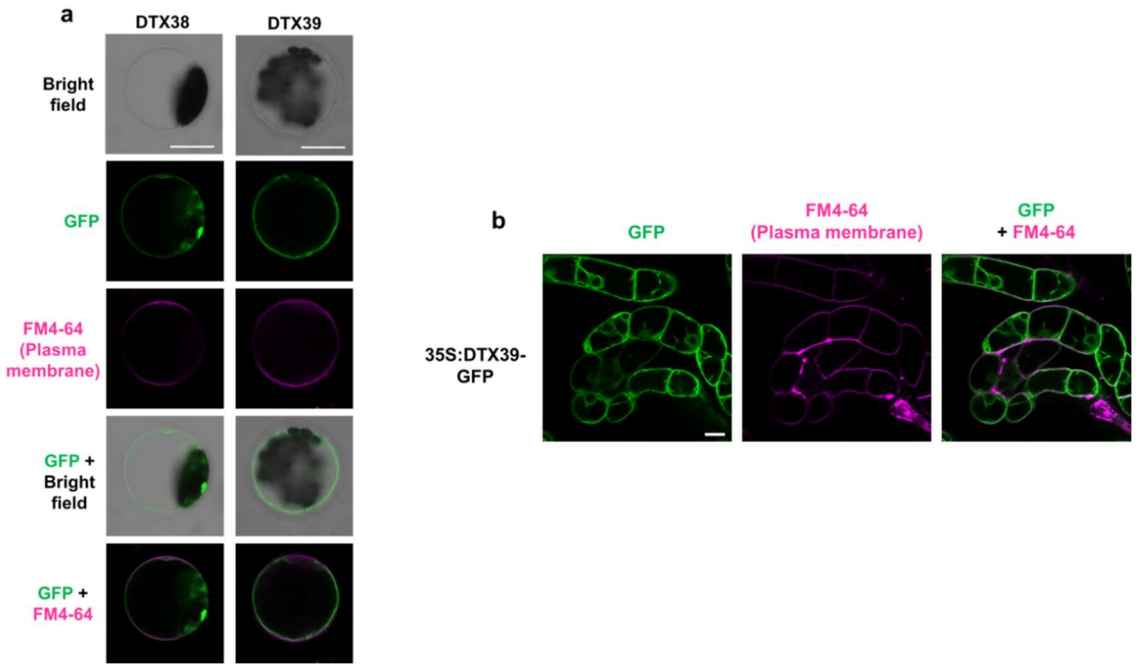

Extended Data Fig. 4. Subcellular localization of DTX38 and DTX39 in *Arabidopsis* protoplasts and BY-2 cells.

a, Confocal and bright field microscope images of *Arabidopsis* leaf mesophyll protoplasts transiently expressing DTX38-GFP or DTX39-GFP, with the plasma membrane stained with FM4-64 fluorescent dye.

b, Confocal microscope images of tobacco BY-2 cells stably expressing DTX39-GFP, with the plasma membrane stained with FM4-64. Scale bars = 20 μm.

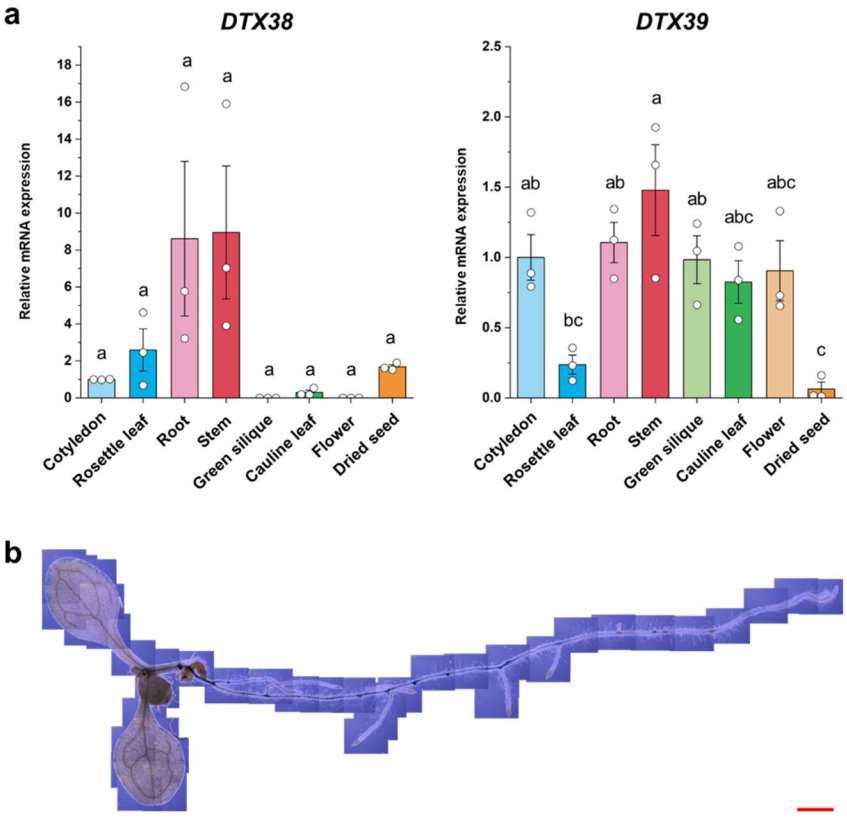

Extended Data Fig. 5. a, Expression of DTX38 and DTX39 genes in different *Arabidopsis* organs.

a, The chart shows mRNA levels measured by qRT-PCR in the cotyledons of 5-day-old seedlings, rosette leaves and roots of 14-day-old seedlings, stems, siliques, cauline leaves, and flowers of 6-week-old plants, and dried seeds. The error bars indicate the standard error (SE) of three biological replications (n = 3). Different lowercase letters indicate significant differences using one-way ANOVA with a Tukey's HSD test ($p < 0.05$).

b, GUS histochemical staining of 7-day-old transgenic *Arabidopsis* seedlings expressing *ProDTX39:GUS*. Scale bar = 1 mm.

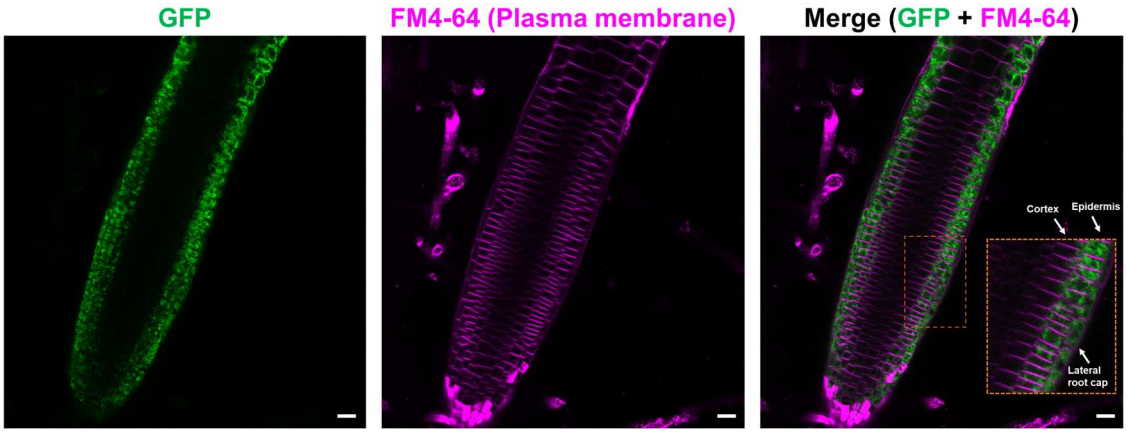

Extended Data Fig. 6. Localization of DTX39-GFP in root tip cells.
The image shows GFP fluorescence signals in the root tip of 14-day-old ProDTX39:DTX39-GFP/ *dtx39-1* transgenic plants. Enlarged images are shown in an orange dotted box. Scale bars = 20 μm.

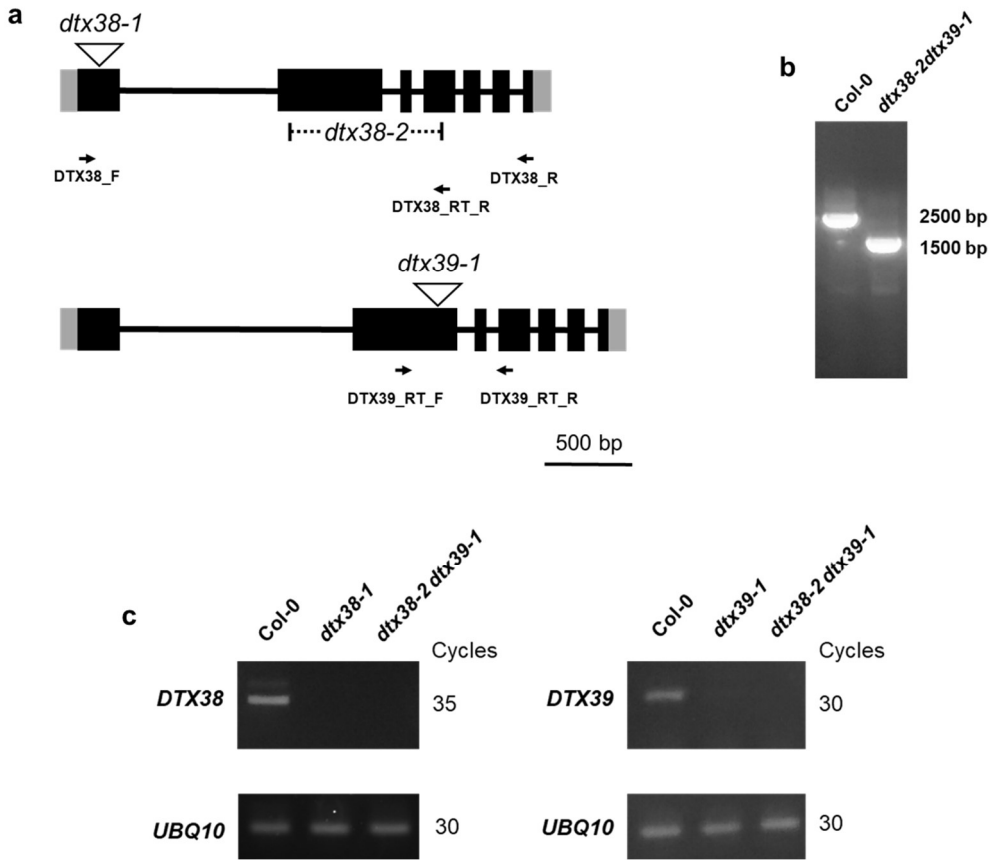

Extended Data Fig. 7. Characterization of *dtx38* and *dtx39* mutants.

a, Schematic diagram showing the *DTX38* and *DTX39* gene structures and the location of *dtx38-1*, *dtx38-2*, *dtx39-1* mutations. Exons and untranslated regions are represented by black and gray boxes, respectively. T-DNA insertion sites in *dtx38-1* (SALK_201145C) and *dtx39-1* (GABI_100G09) mutants are shown as triangles. The dotted line indicates the deleted region in the *dtx38-2* mutant generated by CRISPR-Cas9. Arrows indicate the positions and directions of PCR primers used for the genome PCR and RT-PCR. Oligonucleotide sequences of the primers are listed in the Supplementary Table 3.

b, Genome PCR with primers DTX38_F and DTX38_R shows the *DTX38* gene deletion in the *dtx38-2 dtx39-1* double knockout mutant.

c, RT-PCR analysis of *DTX38* and *DTX39* in the wild type (Col-0), *dtx38-1*, *dtx39-1,* and *dtx38-2 dtx39-1* mutants using the primers indicated in (**a**) (DTX38_F/DTX38_RT_R or DTX39_RT_F/DTX39_RT_R). *UBQ10* serves as an internal control to show the presence of cDNA in the PCR template. The numbers on the right indicate the number of PCR cycles.

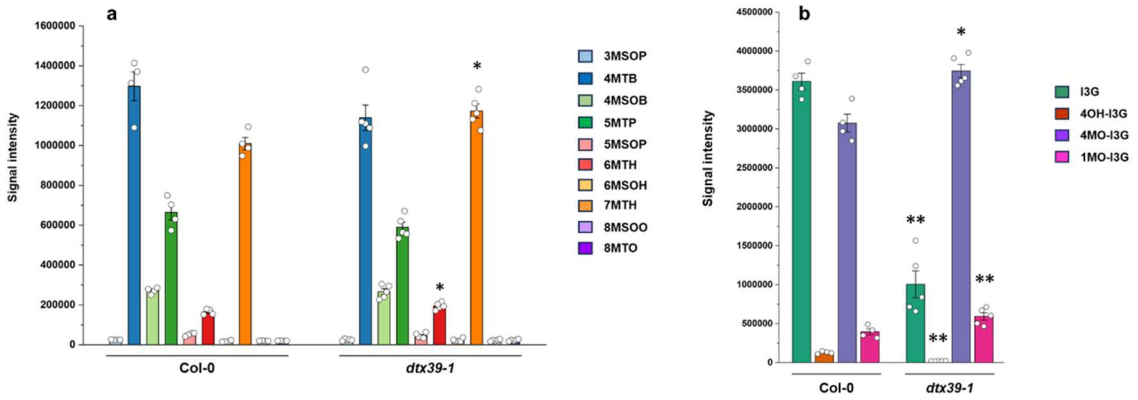

Extended Data Fig. 8. Glucosinolate levels in leaves measured using LC-MS/MS.
a, b, Each aliphatic (**a**) and indolic (**b**) glucosinolate level in the wild type (Col-0) and *dtx39-1* mutant rosette leaves at 14 days. 3MSOP, 3-Methylsulfinylpropyl; 4MTB, 4-Methylthiobutyl; 4MSOB, 4-Methylsulfinylbutyl; 5MSOP, 5-Methylsulfinylpentyl; 5MTP, 5-methylthiopentyl; 6MTH, 6-methylthiohexyl; 6MSOH, 6-Methylsulfinylhexyl; 7MTH, 7-methylthioheptyl; 8MSOO, 8-methylslufinyloctyl; 8MTO, 8-methylthiooctyl; I3G, Indol-3-ylmethyl; 4OH-I3G, 4-hydroxyindol-3-ylmethyl; 1MO-I3G, 1-methoxyindol-3-ylmethyl; 4MO-I3G, 4-methoxyindol-3-ylmethyl. Error bars represent the standard error (SE) of four and five replications (n = 4-5). Statistically significant differences between the Col-0 and *dtx39-1* are indicated by *($p < 0.05$) and **($p < 0.01$); Student t-test.

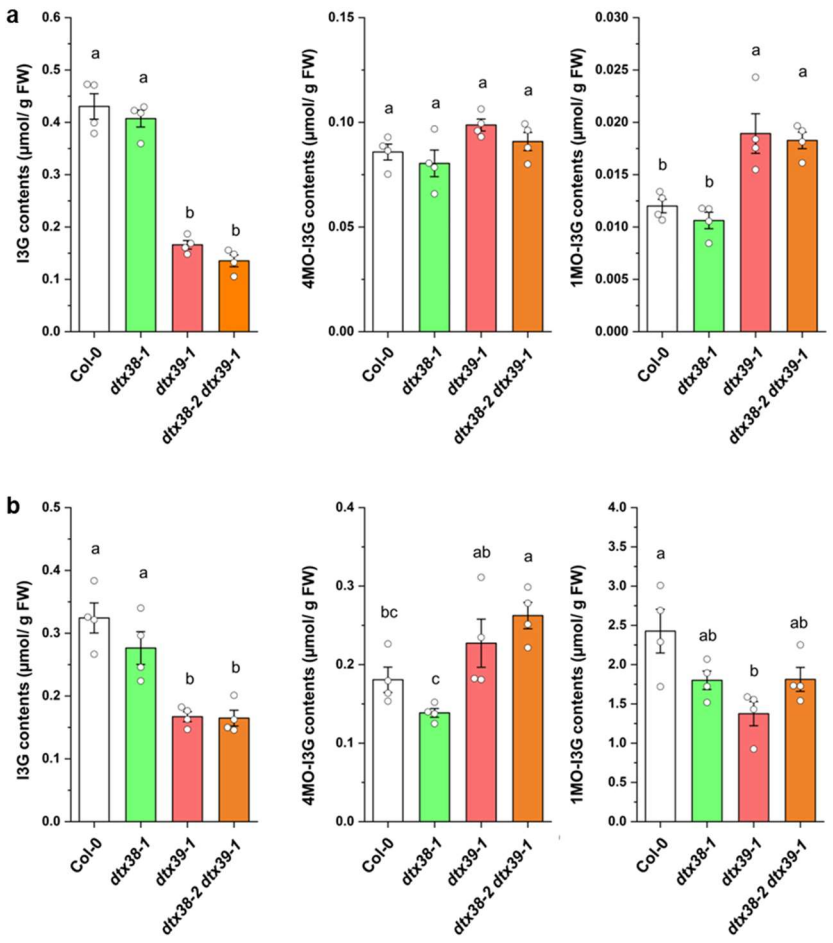

Supplementary Figure 1.
a, b, Magnified chart of each indolic glucosinolate level in leaves (**a**) and roots (**b**) of wild type (Col-0), *dtx38-1*, *dtx39-1*, *dtx38-2,* and *dtx39-1* as shown in Fig. 5**c**,**d**. Error bars represent the standard error (SE) of four biological replications (n = 4). Different lowercase letters indicate significant differences using one-way ANOVA with a Tukey's HSD test ($p < 0.05$).

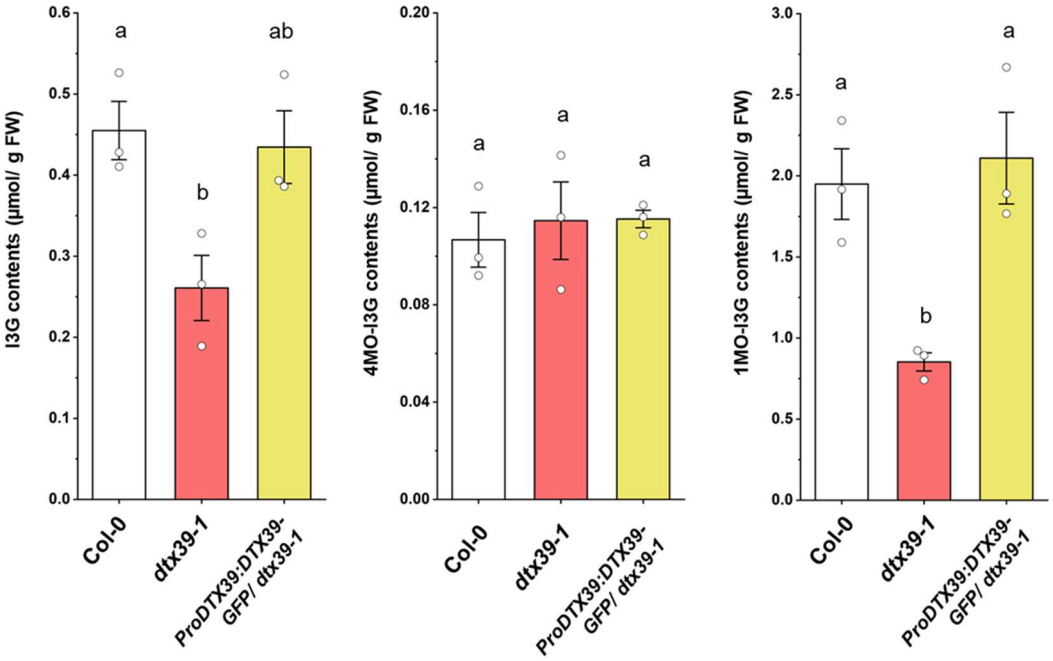

Supplementary Figure 2. Each indolic glucosinolate level in the roots of wild type (Col-0), *dtx39-1* mutant, and a transgenic plant complemented *DTX39-GFP* gene drive by its own promoter (ProDTX39:DTX39-GFP/*dtx39-1*). Error bars represent standard error (SE) of three biological replications (n = 3). Different lowercase letters indicate significant differences using one-way ANOVA with a Tukey's HSD test ($p < 0.05$).

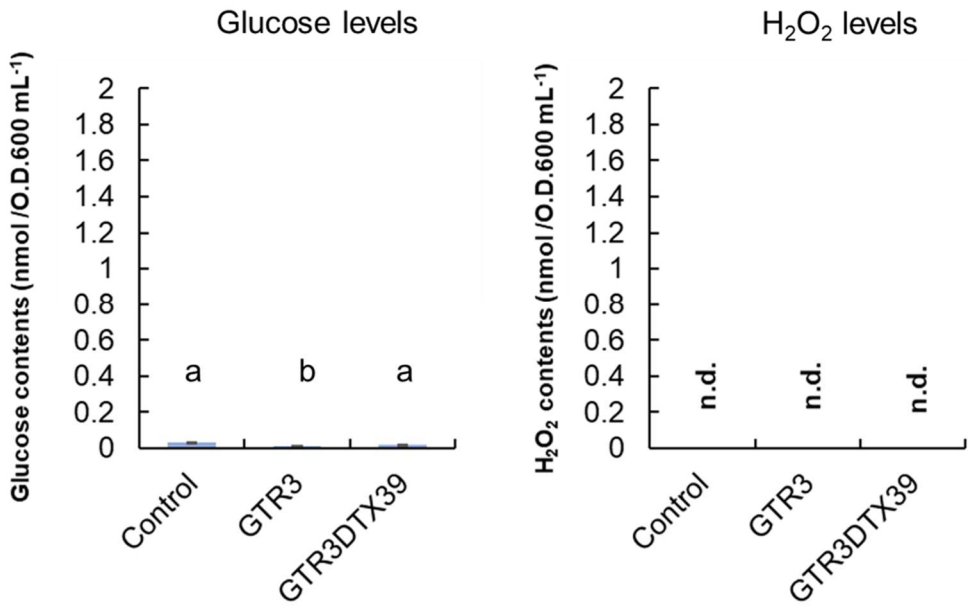

Supplementary Figure 3. Low endogenous glucose and hydrogen peroxide levels in the yeast extracts used for the glucosinolate measurements. The indicated cells were homogenized with MeOH to extract glucosinolate metabolites. The chart shows glucose and hydrogen peroxide levels in the samples without thioglucosidase treatment. Error bars represent the standard error (SE) of three independent experiments (n = 3). Different lowercase letters indicate significant differences using one-way ANOVA with a Tukey's HSD test ($p < 0.05$). 'n.d.' indicates not detected.